

Photochemical & Photobiological Sciences

Accepted Manuscript



This article can be cited before page numbers have been issued, to do this please use: M. V. Rogozina, V. V. Yudanov, R. G. Fedunov, I. P. Pozdnyakov, A. A. Melnikov, S. V. Chekalin and E. Glebov, *Photochem. Photobiol. Sci.*, 2017, DOI: 10.1039/C7PP00299H.



This is an Accepted Manuscript, which has been through the Royal Society of Chemistry peer review process and has been accepted for publication.

Accepted Manuscripts are published online shortly after acceptance, before technical editing, formatting and proof reading. Using this free service, authors can make their results available to the community, in citable form, before we publish the edited article. We will replace this Accepted Manuscript with the edited and formatted Advance Article as soon as it is available.

You can find more information about Accepted Manuscripts in the [author guidelines](#).

Please note that technical editing may introduce minor changes to the text and/or graphics, which may alter content. The journal's standard [Terms & Conditions](#) and the ethical guidelines, outlined in our [author and reviewer resource centre](#), still apply. In no event shall the Royal Society of Chemistry be held responsible for any errors or omissions in this Accepted Manuscript or any consequences arising from the use of any information it contains.

Cite this: DOI: 10.1039/c0xx00000x

www.rsc.org/xxxxxx

ARTICLE TYPE

Short-Lived Intermediates in Photochemistry of OsCl_6^{2-} Complex in Aqueous Solutions

Marina V. Rogozina^{a,b,*}, Vladislav V. Yudanov^{a,b}, Roman G. Fedunov^b, Ivan P. Pozdnyakov^{a,c}, Alexey A. Melnikov^d, Sergey V. Chekalin^d, Evgeni M. Glebov^{a,c}

Received (in XXX, XXX) Xth XXXXXXXXX 20XX, Accepted Xth XXXXXXXXX 20XX

DOI:

Two mechanisms of $\text{Os}^{\text{IV}}\text{Cl}_6^{2-}$ photolysis were studied by means of the quantum chemical calculations in gas and aqueous phases. The difference between these mechanisms is in the nature of the possible Os(IV) key intermediates (KI). According to calculations, the intermediate is the $\text{Os}^{\text{IV}}\text{Cl}_5^-$ complex of square pyramidal coordination geometry. The calculations do not give an opportunity to make an unambiguous choice between triplet and quintet multiplicities of $\text{Os}^{\text{IV}}\text{Cl}_5^-$. The calculated CASSCF/IMCP-SR1 transition energies for $^5\text{Os}^{\text{IV}}\text{Cl}_5^-$ are lower than for $^3\text{Os}^{\text{IV}}\text{Cl}_5^-$, while the calculated XMC-QDPT2/SBKJC spectra for the triplet state are in better agreement with the experimental absorption spectrum of the KI than for the quintet state.

1. Introduction

Ultrafast dynamics of transition metal complexes is an active area of research in chemical physics [1-9]. Combination of ultrafast (femtosecond), nanosecond and stationary experimental data accompanied by quantum chemical calculations allows one to identify the short-living intermediates and to construct the verified reaction mechanism.

Recently, we have reviewed the efforts in studying primary photophysical and photochemical processes for hexahalide complexes of tetravalent ions of platinum group metals (see [10] and references there). Five complexes of this type were the subjects of femtosecond studies, namely, $\text{Pt}^{\text{IV}}\text{Cl}_6^{2-}$, $\text{Pt}^{\text{IV}}\text{Br}_6^{2-}$, $\text{Ir}^{\text{IV}}\text{Cl}_6^{2-}$, $\text{Ir}^{\text{IV}}\text{Br}_6^{2-}$, and $\text{Os}^{\text{IV}}\text{Br}_6^{2-}$. Among them, the photophysics and photochemistry of $\text{Pt}^{\text{IV}}\text{Br}_6^{2-}$ in aqueous and alcoholic solutions is experimentally examined in the time range from absorption of a light quantum to the formation of final photolysis products, and supported by quantum chemistry [11, 12]. In aqueous solutions the only photochemical process is photoaquation [13, 14]. It was shown that the main reactive intermediate is the pentacoordinated PtBr_5^- complex in the singlet state [11].

For other mentioned complexes, the mechanisms are not as complete as for $\text{Pt}^{\text{IV}}\text{Br}_6^{2-}$. For $\text{Pt}^{\text{IV}}\text{Cl}_6^{2-}$ the overall photochemical process is also photoaquation, yielding the $\text{Pt}^{\text{IV}}\text{Cl}_5(\text{H}_2\text{O})^-$ complex at the first stage [15]. The mechanism includes redox reactions with the participation of short-lived Pt(III) intermediates [16]. As a result, the chain pathway of solvation is realized in aqueous [15] and acetonitrile [17] solutions. Identification of Pt(III) intermediates was based on the X_α calculations performed by Goursot et al. in the 80th years of XX century [18]. No verification of results by modern quantum chemical methods was done.

Low quantum yields of $\text{Ir}^{\text{IV}}\text{Cl}_6^{2-}$ photolysis in aqueous

solutions [19] did not allow one to correlate photochemical [20] and photophysical [21] pulsed experiments, as there were no observable precursors of the stable photoproducts.

Photochemistry of $\text{Os}^{\text{IV}}\text{Br}_6^{2-}$ in aqueous and methanolic solutions is similar to the case of $\text{Pt}^{\text{IV}}\text{Br}_6^{2-}$ [11, 12]. The difference is that the ground state of the pentacoordinated intermediate $\text{Os}^{\text{IV}}\text{Br}_5^-$ is triplet, while for the case of PtBr_5^- it is singlet. Additional data on the stationary and nanosecond laser flash photolysis of $\text{Os}^{\text{IV}}\text{Br}_6^{2-}$ are required to complete its photolysis mechanism.

No chemical reactions were detected in aqueous $\text{Ir}^{\text{IV}}\text{Br}_6^{2-}$ solutions upon ultrafast excitation at 770 nm [12], unlike the gas phase photodissociation of the complex [22]. Actually, very little is known about photochemistry of $\text{Ir}^{\text{IV}}\text{Br}_6^{2-}$, with additional complications due to its instability in the absence of free Br^- anions.

Recently we examined ultrafast processes for the pseudohexahalide complex $\text{Pt}^{\text{IV}}(\text{SCN})_6^{2-}$ [23]. Its photophysics and photochemistry were found to be similar to those of $\text{Pt}^{\text{IV}}\text{Br}_6^{2-}$.

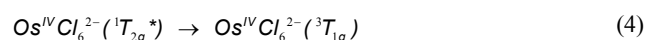
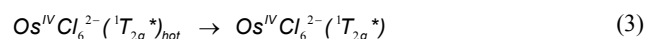
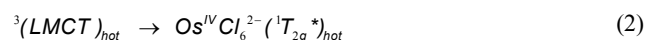
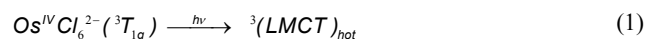
In addition to the mentioned hexahalide complexes of platinum metals, we have recently performed experiments on ultrafast spectroscopy of $\text{Os}^{\text{IV}}\text{Cl}_6^{2-}$ in aqueous solutions [24]. Irradiation of this complex in water [25, 26], methanol [26], acetonitrile and pyridine [25] resulted in photosolvation, while irradiation in chloroform gave rise to photooxidation of Os(IV) to Os(V) [27].

The quantum yield of photoaquation was found to be wavelength-dependent, dropping to the longer irradiation wavelengths [24]. The main result of [24] was the registration of the intermediate (further – key intermediate, KI) with the maximum in the region of 450-470 nm and plateau in the region of 550-650 nm. The characteristic lifetime of the KI is about 20 ps. Because of low quantum yield of photoaquation (0.005 at the irradiation wavelength of 405 nm [24]) the main channel of the

intermediate's decay was identified as the transition to the ground state of $\text{Os}^{\text{IV}}\text{Cl}_6^{2-}$. Two possibilities of the KI identification were proposed [24]: either the lowest electronic excited state of $\text{Os}^{\text{IV}}\text{Cl}_6^{2-}$ or pentacoordinated complex of $\text{Os}(\text{IV})$, $\text{Os}^{\text{IV}}\text{Cl}_5^-$ situated in the solvent cage with the chloride anion. Based on analogy with photophysics of $\text{Os}^{\text{IV}}\text{Br}_6^{2-}$ [11, 12], it was proposed that the ground state of $\text{Os}^{\text{IV}}\text{Cl}_5^-$ is most likely triplet.

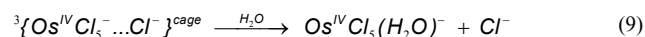
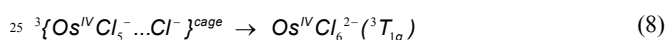
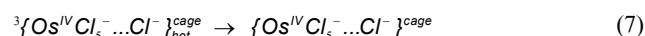
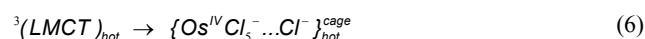
Corresponding to the way of the KI identification, two possible tentative mechanisms of $\text{Os}^{\text{IV}}\text{Cl}_6^{2-}$ photoaquation were presented in [24]. In the following equations, $\text{Os}^{\text{IV}}\text{Cl}_6^{2-}$ was considered as the octahedral low-spin complex [28]. In this case, ground state and lowest electronic excited state of $\text{Os}^{\text{IV}}\text{Cl}_6^{2-}$ are ${}^3\text{T}_{1g}$ and ${}^1\text{T}_{2g}$ correspondingly [29].

Mechanism 1 (KI is the lowest electronic excited state of $\text{Os}^{\text{IV}}\text{Cl}_6^{2-}$, namely $\text{Os}^{\text{IV}}\text{Cl}_6^{2-}({}^1\text{T}_{2g}^*)$)

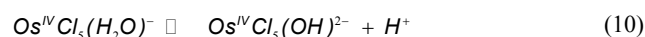


where ${}^3(\text{LMCT})$ is the initially formed excited state.

Mechanism 2 (KI is the ionic pair $\{\text{Os}^{\text{IV}}\text{Cl}_5^- \dots \text{Cl}^-\}_{\text{cage}}$)



The $\text{Os}^{\text{IV}}\text{Cl}_5(\text{H}_2\text{O})^-$ complex demonstrates acidic properties [24]:



When $\text{Os}^{\text{IV}}\text{Cl}_6^{2-}$ is irradiated in the solutions with neutral pH, equilibrium (10) is right-shifted, and the $\text{Os}^{\text{IV}}\text{Cl}_5(\text{OH})^{2-}$ hydroxocomplex is the product of photoaquation [24].

In this work we describe our efforts in identification of the KI by means of quantum chemical calculations.

2. Experiment and quantum chemical calculations

Ultrafast spectroscopy. In this work we analyze the results obtained using the experimental setup described in detail in [30]. The samples were excited by ~ 60 fs pulses (energy ca. 1 μJ , pulse repetition rate 1 kHz) at ~ 400 nm (second harmonic of a Ti:sapphire generator-amplifier system, CDP Ltd., Moscow, Russia). 200 pulses were used to record a single time-resolved spectrum. Each kinetic curve contained 110 points (60 points with a 100 fs step, 20 points with a 500 fs step, and 30 points with a 3 ps step). The investigated solutions (total volume of 20 ml) were pumped through a 1 mm cell at room temperature to provide uniform irradiation and avoid possible degradation due to photochemical reactions. The experimental data were globally fitted by a three-exponential model. The fitting program

performed corrections of the group velocity dispersion and calculated the response time of the instrument.

Quantum chemical calculations. Ground-state gas-phase geometry optimization was performed at the Hartree-Fock level of theory (RHF, ROHF, UHF) using the SBKJC, Def2-TZVP, IMCP-NR1 and IMCP-SR1 basis sets [31, 32]. The calculations were carried out using the GAMESS-US package [33] for the Def2-TZVP, IMCP-NR1 and IMCP-SR1 basis sets and FireFly version 8.1.1 [34] for the SBKJC basic set. Effect of solvent (water) was taken into account at the framework of the polarizable continuum model (PCM).

In the course of GAMESS-US package calculations, electronic excitation terms were computed at the complete active space configuration interaction (state-specific CASSCF) with 8 active orbitals and 10 active electrons using the same basis sets. When SCF convergence failure happened the active space was lowered to 6 active orbitals and 6 active electrons.

In the course of FireFly calculations, electronic spectra were computed at the framework of Extended Multi-Configuration Quasi-Degenerate Perturbation Theory (XMCQDPT) [34] with the same active space (state-averaged CASSCF). All the molecular systems were calculated with prescribed multiplicity and total electronic charge.

3. Results and discussion

3.1. Geometry of ground state and electronic excited states of $\text{Os}^{\text{IV}}\text{Cl}_6^{2-}$

$\text{Os}^{\text{IV}}\text{Cl}_6^{2-}$ is a low spin complex with the $5d^4$ electronic configuration. To clarify the further description, the approximate structure of orbitals (based on the results of Jørgensen [28, 35] obtained in assumption on octahedral symmetry of the complex) is shown in Fig. 1. In the framework of the simple crystal field approach with the O_h symmetry the ground state of $\text{Os}^{\text{IV}}\text{Cl}_6^{2-}$ is triplet (${}^3\text{T}_{1g}$ [29]). In the literature, octahedral symmetry is typically used in the works on $\text{Os}^{\text{IV}}\text{Cl}_6^{2-}$ spectroscopy [28, 29] in spite of the Yahn-Teller distortion to lower symmetry.

Quantum chemical calculations performed in this work resulted in slight distortions from octahedral geometry to the D_{2h} symmetry. The geometrical structure of $\text{Os}^{\text{IV}}\text{Cl}_6^{2-}$ is shown in Fig. 2 (and in Fig. S1 of Supporting Information). Detailed results of calculations performed with different methods are collected in Table S1 of Supporting Information. Two axial Os-Cl bonds are 90° with equatorial plane, and the Cl-Os-Cl bond angles of atoms lying in the equatorial plane may be slightly (not more than 2°) different from 90° for the different methods. Os-Cl bond lengths for singlet and triplet states vary from 2.355 to 2.478 Å. Axial Os-Cl bonds for quintet states (2.65 ÷ 2.73 Å) are sufficiently longer than the covalent Os-Cl bonds. This is an indication of the dissociative character of the quintet states.

All equatorial Os-Cl bond lengths and chlorine charges calculated with one method are close to each other. Typically (with a couple of exclusions), for the triplet states calculated axial Os-Cl bond lengths and chlorine atoms charges are less than corresponding parameters for equatorial chlorine atoms. For singlet states the prevailing picture is opposite. Atomic charges on the axial chlorine atoms for quintet states are more negative than ones on the equatorial chlorines.

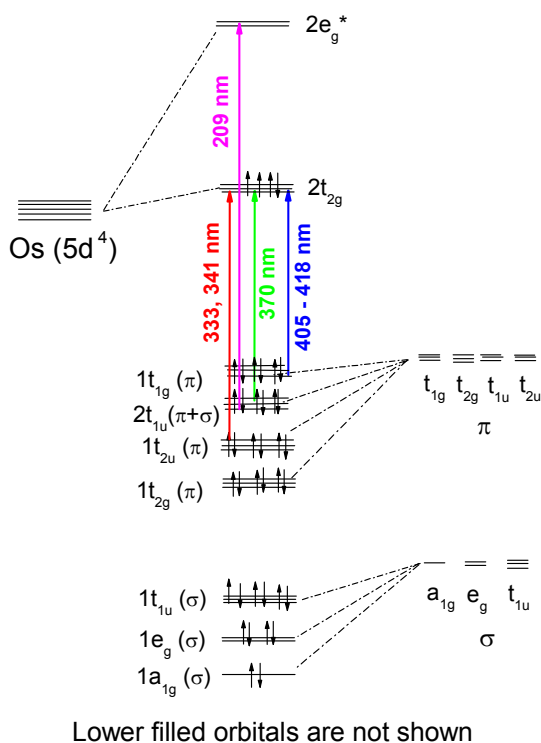


Fig. 1. The structure of molecular orbitals of the OsCl_6^{2-} complex in the framework of O_h symmetry according to [27] (non-relativistic approximation). Arrows correspond to LMCT transitions. Wavelengths of the band maxima are indicated for aqueous solutions.

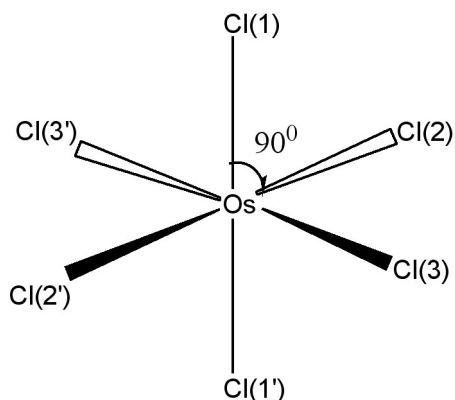


Fig. 2. Geometry of OsCl_6^{2-} ground state according to quantum chemical calculations. For details see Table S1 in Supporting information.

3.2. UV spectrum of $\text{Os}^{\text{IV}}\text{Cl}_6^{2-}$

UV spectrum of $\text{Os}^{\text{IV}}\text{Cl}_6^{2-}$ in aqueous solutions (pH \sim 7) is shown in Fig. 3 (black line). We use here the molar absorption coefficients obtained in [24], which are close to that of reported by Jørgensen [28].

The interpretation of absorption bands of the initial complex in the framework of octahedral symmetry (according to [28]) is presented in Fig. 1. A low intense band appeared as a shoulder in the region of 405 - 418 nm was assigned to an LMCT transition. According to Jørgensen interpretation [28, 35] these band corresponds to the $\pi_{\text{Cl}}(t_{1u}) \rightarrow \text{Os}(t_{2g})$ promotion. The LMCT bands in the region of 320-375 nm are represented by a doublet

($\lambda_{\text{max}} = 333$ and 341 nm) and a single band with a maximum at 370 nm. These bands correspond to $\pi_{\text{Cl}}(t_{2u}) \rightarrow \text{Os}(t_{2g})$ and $(\pi+\sigma)_{\text{Cl}}(t_{1u}) \rightarrow \text{Os}(t_{2g})$ promotions [28]. The most intense LMCT band at 210 nm was assigned to the $\pi_{\text{Cl}} \rightarrow \text{Os}(e_g)$ promotion [28]. Low intense bands in the regions of 301, 278 and 255 nm were interpreted by the d-d transitions [28]; they are partially superimposed with the LMCT bands.

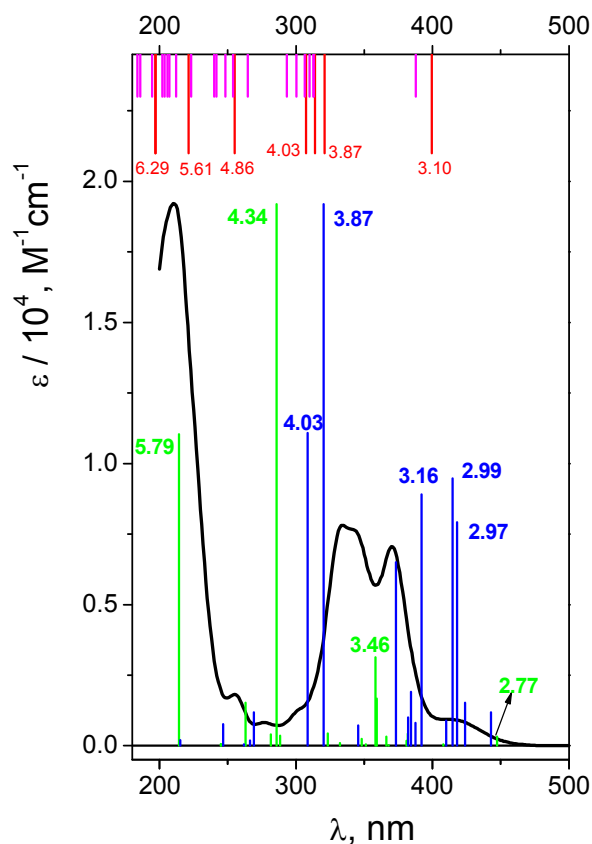


Fig. 3. Electronic absorption spectrum of $\text{Os}^{\text{IV}}\text{Cl}_6^{2-}$ in aqueous solution (black line) and the results of calculations. Red lines - (CASSCF(8,10)/IMCP-SR1, $M = 3$) calculations (gas phase); magenta lines - CASSCF(8,10)/IMCP-SR1, $M = 3$ /PCM(water) calculations; green lines - XMCQDPT(10,8)/SBKJC calculations (gas phase); blue lines - XMCQDPT(10,8)/SBKJC/PCM calculations (water). For CASSCF calculations oscillator strengths are not available. For XMCQDPT calculations oscillator strengths are normalized to the maximal experimental absorption (at 209 nm). Energies of principal transitions (in eV) are specified.

In spite of the undoubted interpretation of $\text{Os}^{\text{IV}}\text{Cl}_6^{2-}$ electronic absorption spectrum in the literature, we have performed its quantum chemical calculations. The necessity of these calculations stems from the use of quantum chemistry for the assignment of short-lived reactive intermediates of Os(IV) in this work. Before using calculations for the assignment of the absorption bands obtained in time-resolved experiments, we had to ensure that the calculated spectrum of $\text{Os}^{\text{IV}}\text{Cl}_6^{2-}$ ground state did not contradict to the experimental one.

Calculations of excited states energy levels were performed by

different methods using GAMESS-US package (by means of CASSCF(8,10)/IMCP-SR1, CASSCF(8,10)/IMCP-NR1, and CASSCF(8,10)/Def2-TZVP methods) and FireFly package. In the case of GAMESS calculations the oscillator strengths could not be figured out, while in the case of FireFly calculations it was possible. The results of calculations of energies and orbital populations are presented in Supporting Information. Tables S2 and S3 contain the gas phase data obtained from GAMESS-US and FireFly calculations, while Tables S4 and S5 contain the results of calculations performed in aqueous phase.

The excitation energies obtained by GAMESS and FireFly calculations in gas phase using different basis sets are shown schematically in Fig. 4. Only for the triplet ground state the results of calculations are comparable with the experimental spectrum. The calculations performed in basis sets IMCP-SR1 (triplet manifold) and SBKJC give the best agreement between the calculated excitation energies and the experimentally observed spectra. Thus further analysis has been carried out only with these basis sets. These calculations are represented in Fig. 3 as red vertical lines under the upper scale (CASSCF(10,8)/IMCP-SR1) and green vertical lines above the lower scale (SBKJC).

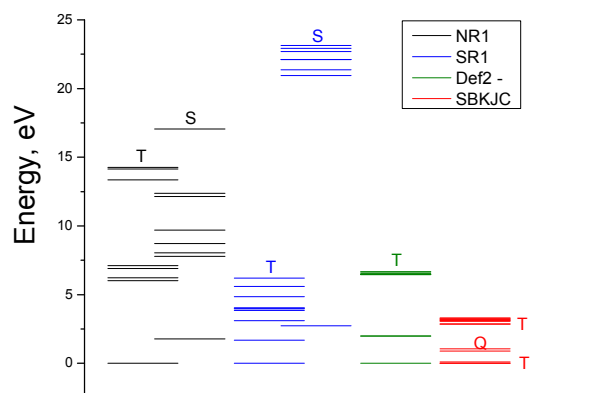


Fig. 4. Results of GAMESS and FireFly calculations of $\text{Os}^{\text{IV}}\text{Cl}_6^{2-}$ spectrum (gas phase) using different basic sets. Abbreviations NR1, SR1, T, SR1, Def2 and SBKJC correspond to CASSCF(8,10)/IMCP-NR1, CASSCF(8,10)/IMCP-SR1, CASSCF(8,10)/Def2-TZVP and SBKJC basic sets correspondingly. Multiplicity of levels is indicated.

Let us analyze the results of the IMCP-SR1 calculations. First of all, to evaluate the possible solvent effect, calculations in the framework of PCM with 32 excited states were performed (see Table S4 of Supporting Information). The results are shown in Fig. 3 (magenta vertical lines under the upper scale). Consideration of the solvent in calculation reduces molecular symmetry, resulting in increasing the number of spectral lines that complicates the analysis of transitions. In spite of that, one can see that the difference between the results of gas phase and aqueous solutions calculations is not large. This is true both for structures (Table S1 of Supporting information) and spectra (Fig. 3, upper scale). For these reasons, further analysis was performed only for the results obtained in the gas phase.

Let us compare the experimental (Fig. 3) and calculated (Fig. 3 and Table S2 of Supporting information) spectra. The lowest energy band (T1 \rightarrow T2) was assigned to an electron

transfer from HOMO (picture of active orbitals see Fig. S2) including only $d_{yz}(\text{Os})$ atomic orbital to LUMO composed by d_{xx} , d_{yy} , $d_{zz}(\text{Os})$ and $p_x(\text{Cl}(2, 2'))$ atomic orbitals. Calculated energy for this transition is 3.1 eV (399 nm), which corresponds to the shoulder in the experimental spectrum. The group of transitions from T1 to T3, T4 and T5 with energies 3.86, 3.95 and 4.03 eV (321, 314 and 307 nm) is mainly constituted from the same atomic orbitals as (T1 \rightarrow T2) transition, but with slightly different occupancies. These transitions could be put in compliance to LMCT bands in the region of 320-370 nm in the experimental spectrum. Further, triplet level T7 with energy equal to 5.6 eV (221 nm) could be assigned as (LUMO+1) orbital. States T6, T8 and T9 with energies 4.86, 6.29 and 6.30 eV (255 and 197 nm) are constituted from HOMO, LUMO and (LUMO + 1) orbitals with different populations. Transitions from (T1 \rightarrow T6) to (T1 \rightarrow T9) could be considered as responsible for the most intense LMCT band at 210 nm and the low intense band at 255 nm. Therefore, (CASSCF(8,10)/IMCP-SR1, M = 3) calculations do not contradict to the experimental spectrum (but note that the absence of oscillator strengths allows one to make only tentative conclusions).

Now let us consider the results of XMCQDPT(10,8)/SBKJC calculations. Gas phase FireFly calculations are presented as green vertical lines in Fig. 3 (see also Table S3 in Supporting Information). The oscillator strengths were normalized to the maximal value of the molar absorption coefficient of the experimental spectrum (green vertical line at 4.34 eV (286 nm) in Fig. 3). The XMCQDPT (10,8)/SBKJC/PCM(water) spectrum is presented in Fig. 3 as blue vertical lines. The oscillator strengths were normalized to the maximal value of the molar absorption coefficient of the experimental spectrum (blue vertical line at 3.87 eV (320) nm in Fig. 3).

The impact of solvent on the position of the spectral lines is ambiguous (Fig. 3 and Table S5 of Supporting Information). The line corresponding to the highest energy is shifted to shortwave region all other lines are shifted to the longwave region. Apparently this is because the whole range was narrower compared to the spectrum calculated in the gas phase, although the shape of the spectrum in water qualitatively matches the shape of the spectrum in the gas phase. There is some difference; the additional line at 3.16 eV (392 nm) is appeared to be at the left from the doublet 2.99, 2.97 eV (415, 418 nm). The following analysis was performed for the gas phase spectrum (Table S3 in Supporting information).

The first energy band with nonvanishing oscillator strength (T1 \rightarrow T4) was assigned to an electron transfer from HOMO-2 including $d_{yz}(\text{Os})$ main atomic orbitals to LUMO including following main atomic orbitals: d_{yz} , d_{yy} , $d_{zz}(\text{Os})$ and $p_y(\text{Cl}(5, 4))$, $p_z(\text{Cl}(3, 2))$. Calculated energy for this transition is 2.77 eV (447 nm), which corresponds to the shoulder in the experimental spectrum (Fig. 3).

The interim energy band for transition (T1 \rightarrow T11) (3.46 eV, 358 nm) was assigned to the electron transfer from the composition of HOMO-2 and HOMO to the composition of LUMO and LUMO + 1 of average molecular orbitals. Main atomic orbitals in HOMO include $d_{xy}(\text{Os})$ and $d_{xz}(\text{Os})$ parts. The composition of both LUMO and LUMO+1 for the T11 state includes the following main atomic orbitals: d_{xy} , $d_{xz}(\text{Os})$, $p_y(\text{Cl}(1'))$ for LUMO and d_{yy} , $d_{zz}(\text{Os})$, $p_y(\text{Cl}(3, 3'))$, $p_z(\text{Cl}(2, 2'))$ for LUMO + 1.

The energy band with maximal oscillator strength (T1 \rightarrow T17)

(4.34 eV, 286 nm) was assigned to the electron transfer from the composition of HOMO-2, HOMO-1 and HOMO to the composition of LUMO and LUMO + 1 of averaged molecular orbitals. HOMO and HOMO-2 were described earlier, and HOMO-1 consists of $d_{xy}(\text{Os})$, $d_{xz}(\text{Os})$ and small part of $p_z(\text{Cl}(1, 1'))$ atomic orbitals. The LUMO orbital for T17 state is the same as LUMO orbital for T11 state but with excluding part of $p_y(\text{Cl}(1'))$ orbital and with including $p_x(\text{Cl}(1, 1'))$, $p_y(\text{Cl}(3, 3'))$ orbitals. The LUMO+1 for T17 state includes the following main atomic orbitals: d_{zz} , $d_{yy}(\text{Os})$ and $p_y(\text{Cl}(3, 3'))$, $p_z(\text{Cl}(2, 2'))$. The energy band (T1 \rightarrow T22) (5.79 eV, 214 nm) was assigned to the electron transfer from HOMO-2 to LUMO. The LUMO orbital for T22 state includes the following main atomic orbitals: d_{xx} , d_{yy} , $d_{zz}(\text{Os})$ and $p_x(\text{Cl}(1, 1'))$, $p_y(\text{Cl}(3, 3'))$, $p_z(\text{Cl}(2, 2'))$.

Therefore, we can conclude that both GAMESS and FireFly quantum chemical calculations do not contradict to the experimental spectrum of $\text{Os}^{\text{IV}}\text{Cl}_6^{2-}$ complex. It makes reasonable the use of these types of calculations for the assignment of LMCT states and the short-lived intermediates observed in the course of the ultrafast kinetic spectroscopy experiments.

It should be noted that (CASSCF(8,10)/IMCP-SR1, $M = 3$) calculations predict the existence of low-lying excited quintet (Q_1) and singlet (S_0) energy levels with the energies 1.68 and 2.74 eV above the ground state correspondingly (see Table S2 of Supporting Information). The quintet level, which is dissociative, probably plays a sufficient role in the photolysis mechanism.

3.3. Electronic absorption spectra of possible intermediates of $\text{Os}^{\text{IV}}\text{Cl}_6^{2-}$ photolysis

Results of ultrafast measurements for $\text{Os}^{\text{IV}}\text{Cl}_6^{2-}$ complex in aqueous solutions were analyzed [24] in the framework of the sequential decay of the transient absorption $A \rightarrow B \rightarrow C \rightarrow$ (ground state + products). Intermediate C, which is the precursor of the photoaquation product, was considered as the key intermediate (KI). The Species Associated Differential Absorption Spectra (SADS) of the intermediates were calculated in [24] using formulae derived in [36] (see paragraph "Species Associated Differential Spectra (SADS)" in Supporting Information).

The SADS of the KI obtained in [24] is shown in Fig. 5 (blue dots). Because $\text{Os}^{\text{IV}}\text{Cl}_6^{2-}$ has no significant absorption in the region of probing (440 – 680 nm), the SADS coincides with the electronic absorption spectrum of the KI. According to the shape of the spectrum, there are at least two different absorption bands in the observed wavelength range. The decay of intermediate absorption was described by monoexponential kinetic law with the characteristic lifetime (23 ± 3) ps [24].

Let us discuss the possibility of KI interpretation as one of the lowest electronic absorption state of $\text{Os}^{\text{IV}}\text{Cl}_6^{2-}$. According to (CASSCF(8,10)/IMCP-SR1, $M = 3$) calculations (Table S2 of Supporting Information) the three lowest electronic excited states have different multiplicity. They are quintet Q_1 , singlet S_0 and triplet T_2 states, which energies are 1.7, 2.7 and 3.1 eV above the ground state T_1 .

Wavelengths of possible transitions from Q_1 to another quintet states Q_2 and Q_3 are shown in Fig. 5 as red lines above the bottom axis. One can see that the position of the lowest $Q_1 \rightarrow Q_2$ transition lies in the range of the observed spectrum, and the second band $Q_1 \rightarrow Q_3$ is far in the UV region. As a matter of fact,

the description of the KI spectrum given by transitions within quintet manifold cannot be considered as satisfactory.

Possibility of KI interpretation as the lowest singlet state S_0 should be ruled out, because calculations do not show any transitions from S_0 to other singlet states in the visible and near UV spectral range.

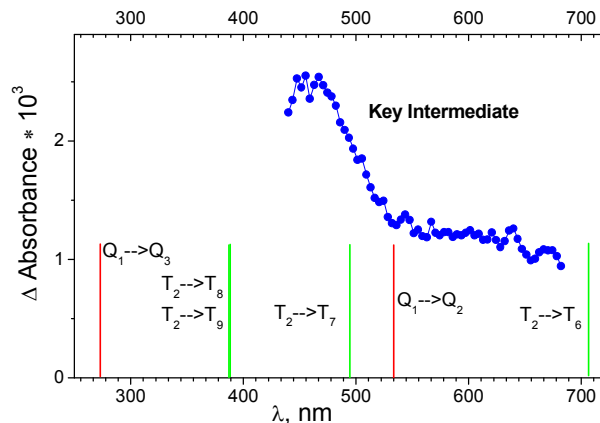


Fig. 5. Blue dots - Species associated difference spectrum (SADS) of the Key Intermediate recorded in ultrafast kinetic spectroscopy experiment ($\lambda_{\text{pump}} = 400$ nm) with $\text{Os}^{\text{IV}}\text{Cl}_6^{2-}$ (2.3×10^{-4} M) in aqueous solution (taken from [24]). Lines above the bottom axis mark positions of possible transitions from the lowest quintet (red lines) and triplet (green lines) electronic excited states of $\text{Os}^{\text{IV}}\text{Cl}_6^{2-}$ (for details see Table S2 of Supporting Information).

Wavelengths of transitions from the lowest excited triplet state T_2 to another triplet states are shown in Fig. 5 as green lines above the bottom axis. One can see that the transitions inside the set of triplet energy levels can provide better description of the experimental spectrum than transitions inside the set of quintet levels. Nevertheless, the possibility of T_2 state partial stabilization (the lifetime of KI is 23 ps, as was mentioned) seems improbable.

Finally, we can conclude that calculations do not support the interpretation of KI as one of the lowest electronic excited states of $\text{Os}^{\text{IV}}\text{Cl}_6^{2-}$, and Mechanism 1 seems improbable. On the other side, the dissociative character of the lowest excited state Q_1 allows one to consider it as a precursor of the ion pair in Mechanism 2.

The pentacoordinated intermediate $\text{Os}^{\text{IV}}\text{Cl}_5^-$ plays the key role in Mechanism 2. GAMESS calculations with the use of the IMCP-SR1 basis set show the existence of two modifications of $\text{Os}^{\text{IV}}\text{Cl}_5^-$ (Fig. 6 and also Fig. S3 of Supporting Information). The first modification (Fig. 6a) is further marked as $\text{Os}^{\text{IV}}\text{Cl}_5^-$ (planar). It was obtained from the $\text{Os}^{\text{IV}}\text{Cl}_6^{2-}$ complex by removal of one chlorine atom lying in equatorial plane. The second modification (Fig. 6b) marked as $\text{Os}^{\text{IV}}\text{Cl}_5^-$ (axial) was obtained by detachment of one axial chlorine atom. Detailed results of geometry calculations performed for both planar and axial modifications are collected in Tables S6a, S6b of Supporting Information. The $\text{Os}^{\text{IV}}\text{Cl}_5^-$ complex in the singlet state tends to trigonal bipyramidal coordination geometry and in triplet state to square pyramidal coordination geometry.

Optimization of all geometrical parameters of $\text{Os}^{\text{IV}}\text{Cl}_5^-$ (axial) was carried out at a low C_1 symmetry. Under optimization of the geometrical parameters for $\text{Os}^{\text{IV}}\text{Cl}_5^-$ (planar) complex a high degree of symmetry (D_{3h}) was preserved only for the singlet state.

In the triplet state the SCF procedure fails for the given high symmetry. Therefore, optimization of geometrical parameters of $\text{Os}^{\text{IV}}\text{Cl}_5^-$ (planar) complex was carried out at a predetermined low C_1 symmetry with fixed values of the Cl-Os-Cl angles in the equatorial plane. For this reason, the electronic structure of planar modification in the triplet state is similar to the electronic structure of axial modification in the triplet state. That is manifested in the asymmetric distribution of charges on the chlorine atoms in the equatorial plane as well as in different bond lengths between osmium and equatorial chlorine atoms (Tables S6a, S6b). The similar result was obtained for the quintet state. After optimization of geometry, the quintet state of $\text{Os}^{\text{IV}}\text{Cl}_5^-$ (planar) complex in fact transits to the axial configuration with the low C_1 symmetry.

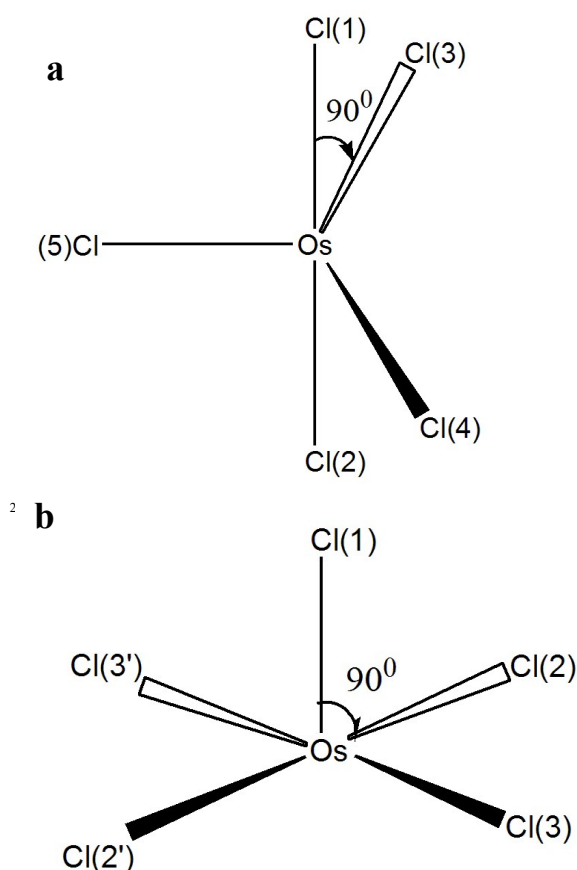
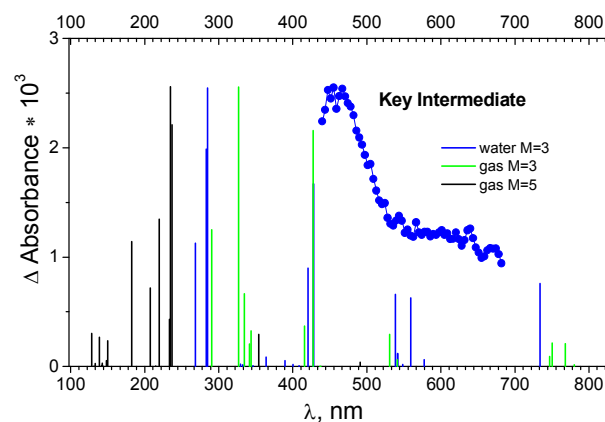


Fig. 6. Planar (a) and axial (b) modifications of $\text{Os}^{\text{IV}}\text{Cl}_5^-$.

Therefore, GAMESS calculations show that the singlet state of $\text{Os}^{\text{IV}}\text{Cl}_5^-$ can exist both of planar and axial configurations, while for the triplet and quintet states only the low symmetry axial configuration is realized. That is why the FireFly calculations for triplets and quintets were performed only for $\text{Os}^{\text{IV}}\text{Cl}_5^-$ (axial) modification. FireFly calculations performed in SBKJC basis set are in accordance with GAMESS results. The geometrical and electronic structures are shown in Table S7.

The electronic absorption spectra of $\text{Os}^{\text{IV}}\text{Cl}_5^-$ with different multiplicities were calculated in FireFly package only (because FireFly provides oscillator strengths). The results of gas phase calculations for the triplet and quintet states are collected in Tables S8 and S9 of Supporting Information correspondingly. Table S10 of Supporting information gives the results of calculation for $^3\text{Os}^{\text{IV}}\text{Cl}_5^-$ in aqueous solutions. Comparison of calculated spectra of the possible pentacoordinated intermediates and the experimental spectrum of the KI is provided by Fig. 7.



40

Fig. 7. Blue dots - Species associated difference spectrum (SADS) of the Key Intermediate recorded in ultrafast kinetic spectroscopy experiment ($\lambda_{\text{pump}} = 400 \text{ nm}$) with $\text{Os}^{\text{IV}}\text{Cl}_5^-$ ($2.3 \times 10^{-4} \text{ M}$) in aqueous solution (taken from [24]). Lines above lower axes mark positions of possible transitions from the lowest quintet and triplet electronic excited states of $\text{Os}^{\text{IV}}\text{Cl}_5^-$ according to calculations.

The XMCQDPT (10,8)/SBKJC in gas phase in the triplet and quintet states are shown in Fig. 7 as vertical green and black lines. The singlet state $\text{Os}^{\text{IV}}\text{Cl}_5^-$ spectra is not shown, because transition energy is 8.51 eV for the axial configuration and exceeds 21.96 eV for the planar configuration. One can see that the spectrum in the triplet state has two pronounced peaks, shifted to the short wavelength region relative to the experimental maximum. Several lines of smaller intensity in the longer wavelength region form the shoulder of the spectrum, which qualitatively coincides with the experimental spectrum. The XMCQDPT (10,8)/SBKJC/PCM(water) in aqueous phase in the triplet state spectrum are presented in Fig. 7 as blue vertical lines.

The calculated energies of different $\text{Os}^{\text{IV}}\text{Cl}_5^-$ modifications are collected in Tables S8-S10 of Supporting Information. The axial modification for the triplet state is characterized by the lowest total energy among all triplet modifications (the UHF/IMCP-SR1 result should be excluded from consideration because the wave function has a high degree of spin contamination, $S^2=3.05$). Indeed, for the quintet state the axial modification is characterized by lower energy than the planar modification. Thus, both for the quintet and triplet states the axial modification is energetically more favorable, whereas for the singlet state it is energetically favorable to be in the planar modification.

Table S8 (Supporting information) shows that for the triplet, the total energy (CASSCF) of the ground state T1 is -4465.532

eV, and for quintet the energy (CASSCF) of the Q1 state is -4465.50 eV (Table S9), there is a slight difference. Including additional electron correlation (XMC-QDPT2 energy of transition) gives the picture similar to the GAMESS calculations, where the quintet is lower in energy than the triplet. GAMESS calculations (Table S6b) show that the quintet is indeed lower in energy than the triplet, but the difference is not much. At the same time, the qualitative coincidence with the experimental spectrum in FireFly (Fig. 7) for the triplet state is much better than for the quintet state (especially in the aqueous phase).

Additional calculations were performed by both methods for the free Os⁴⁺ cation (Table S11 of Supporting information). The results show that the state with multiplicity M = 5 is the most energetically favorable. As can be seen from the previous calculations, the presence of six ligands makes the state M = 3 in Os^{IV}Cl₆²⁻ more favorable. We can assume that the removal of one Cl⁻ anion reduces the influence of the ligands on the electronic structure of the ion Os⁴⁺. Thus, the quintet state could also be expected to be the most favorable in the Os^{IV}Cl₅⁻ complex.

As a result, we conclude that the Os^{IV}Cl₅⁻ complex for sure is the key intermediate of the Os^{IV}Cl₆²⁻ photoaquation. As for the multiplicity of the Os^{IV}Cl₅⁻ ground, both M = 3 and M = 5 cases could not be ruled out from the results of calculations.

Conclusions

In this work the quantum chemical calculations were performed to determine the nature of the key intermediate (KI) of the Os^{IV}Cl₆²⁻ complex photoaquation.

The calculations were carried out using a program packages FireFly 8.1 and GAMESS-US both in gas and aqueous phases. Different methods were used; the best fitting to the experimental data was obtained by means of CASSCF(8,10) method with the basis sets IMCP-SR1 (GAMESS-US) and SBKJC (FireFly).

The geometric and electronic structures and spectra were obtained for the initial Os^{IV}Cl₆²⁻ complex and the Os^{IV}Cl₅⁻ complex as the probable KI. Analysis of electronic transitions and absorption spectra indicates the possibility of reaction of Os^{IV}Cl₆²⁻ photoaquation through a sequence of stages close to the Mechanism 2 (reactions 6-9).

According to quantum-chemical calculations both in GAMESS and FireFly the KI is Os^{IV}Cl₅⁻ of square pyramidal coordination geometry. As for the multiplicity of its ground state, no unambiguous choice between triplet and quintet state could be done. On the one hand, the calculated electronic absorption spectrum of ³Os^{IV}Cl₅⁻ is closer to the experimental one than the ⁵Os^{IV}Cl₅⁻ spectrum (Fig. 7). On the other hand, the calculated energy of the quintet state seems to be lower than for the triplet state. One can see that according to the results of CASSCF GAMESS calculations the Os^{IV}Cl₅⁻ complex is in the quintet state, while according to FireFly calculations the triplet state is favourable. Perhaps this difference stems from the fact that the used IMCP-SR1 basis set takes into account scalar relativistic pseudopotentials, which are ignored by the SBKJC basis set. This is manifested in the compression of the complex; the bond lengths calculated by the IMCP-SR1 are less than bond lengths calculated by the SBKJC. The results of calculations taking into account relativistic amendments seem to be more reliable. The calculation of the total energy of a free osmium ion with charge Q

= 4 also indicates that the quintet state is more energetically favorable.

The results of CASSCF GAMESS calculations include only the static correlation within the active space. Multireference perturbation theory (such as XMCQDPT) corrects the absolute state energies through inclusion of dynamical correlation. This correction is different for the states of different nature and different multiplicity. As a result, the transition energies and the order of states in CASSCF and XMCQDPT calculations may differ substantially. Thus, XMCQDPT results seem more reliable than CASSCF data. Nevertheless, it should be noted that the differences in total energies determining the order of energy levels is rather small.

Thus we can conclude that the reaction of photoaquation passes through Mechanism 2, and the key intermediate is the Os^{IV}Cl₅⁻ complex either in the triplet or in the quintet state.

It should be noted that the use of the time-consuming methods allowing to take into account the spin-orbit coupling, could change the order of energy levels.

Acknowledgements

The financial support of the Russian Science Foundation (Grant № 15-13-10012) is gratefully acknowledged.

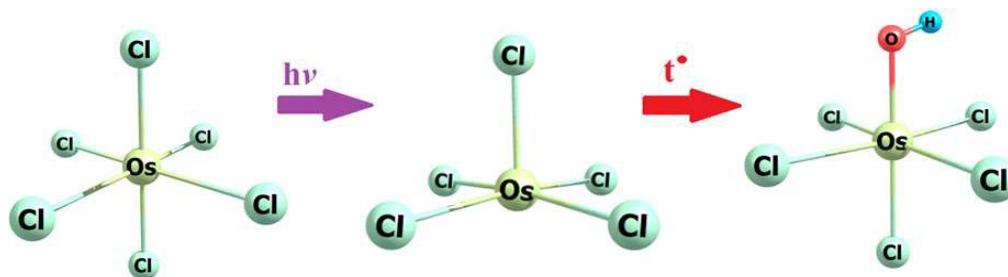
Supporting Information

Supporting information contains the raw data of quantum chemical calculations.

Notes and references

- ^aVoevodsky Institute of Chemical Kinetics and Combustion, 3 Institutskaya Str., 630090, Novosibirsk, Russian Federation; Fax: +7 383 3307350; Tel: +7 383 3309150; E-mail: glebov@kinetics.nsc.ru.
- ^bVologograd State University, 100 University Ave., 400062, Volgograd, Russian Federation; E-mail: rogovina@volsu.ru.
- ^cNovosibirsk State University, 2 Pirogova Str., 630090, Novosibirsk, Russian Federation
- ^dInstitute of Spectroscopy, Russian Academy of Sciences, 5 Fizicheskaya Str., 119333, Troitsk, Moscow, Russian Federation; E-mail: melnikov@isan.troitsk.ru
- 1 A. Vlcek Jr., *Coord. Chem. Rev.*, 2000, **200-202**, 933.
- 2 J.K. McCusker, *Acc. Chem. Res.*, 2003, **36**, 876.
- 3 L.S. Forster, *Coord. Chem. Rev.*, 2006, **250**, 2023.
- 4 E.A. Juban, A.L. Smeigh, J.E. Monat and J.K. McCusker, *Coord. Chem. Rev.*, 2006, **250**, 1783.
- 5 J.N. Schrauben, K.L. Dillman, W.F. Beck and J.K. McCusker, *Chem. Sci.*, 2010, **1**, 405.
- 6 R. Compton, H.K. Gerardi, D. Weidinger, D.J. Brown, W.J. Dressick, E.J. Heilweil and J.C. Owrutsky, *Chem. Phys.*, 2013, **422**, 135.
- 7 J.P. Lomont, S.C. Nguyen and C.B. Harris, *Acc. Chem. Res.*, 2014, **47**, 1634.
- 8 A. Marino, P. Chakraborty, M. Servol, M. Lorenc, E. Collet and A. Hauser, *Angew. Chem. Int. Edit.*, 2014, **53**, 3863.
- 9 C. Sousa, C. de Graaf, A. Rudavskiy, R. Broer, J. Tatchen, M. Etinski and C.M. Marian, *Chem. Eur. J.*, 2013, **19**, 17541.
- 10 E.M. Glebov, I.P. Pozdnyakov, V.F. Plyusnin and I. Khmelinskii, *J. Photochem. Photobiol. C: Photochem. Rev.*, 2015, **24**, 1.

- 11 I.L. Zheldakov, M.N. Ryazantsev and A.N. Tarnovsky, *J. Phys. Chem. Lett.*, 2011, **2**, 1540.
- 12 I.L. Zheldakov, *Ultrafast Photophysics and Photochemistry of Hexacoordinated Bromides of Pt(IV), Os(IV), and Ir(IV) in the Condensed Phase Studied by Femtosecond Pump-Probe Spectroscopy*. Ph. D. Thesis. Bowling Green State University, 2010.
- 13 V. Balzani, M.F. Manfrin and L. Moggi, *Inorg. Chem.*, 1967, **6**, 354.
- 14 E.M. Glebov, V.F. Plyusnin, V.P. Grivin, A.B. Venediktov and S.V. Korenev, *Russ. Chem. Bull.*, 2007, **56**, 2357.
- 15 (a) L.E. Cox, D.G. Peters and E.L. Wehry, *J. Inorg. Nucl. Chem.*, 1972, **14**, 297; (b) K.P. Balashev, V.V. Vasil'ev, A.M. Zimnyakov and G.A. Shagisultanova, *Koord. Khim. (Russian Journal of Coordination Chemistry)*, 1984, **10**, 976 (in Russian); (c) K.P. Balashev, I.I. Blinov and G.A. Shagisultanova, *Zh. Neorg. Khim. (Russian Journal of Inorganic Chemistry)*, 1987, **32**, 2470 (in Russian); (d) I.V. Znakovskaya and E.M. Glebov, *Mendeleev Commun.*, 2016, **26**, 35.
- 16 (a) R.C. Wright and G.S. Laurence, *J. Chem. Soc. Chem. Commun.*, 1972, 132-133; (b) I.V. Znakovskaya, Yu.A. Sosedova, E.M. Glebov, V.P. Grivin and V.F. Plyusnin, *Photochem. Photobiol. Sci.* 2005, **4**, 897; (c) E.M. Glebov, A.V. Kolomeets, I.P. Pozdnyakov, V.F. Plyusnin, V.P. Grivin, N.V. Tkachenko and H. Lemmetyinen, *RSC Adv.*, 2012, **2**, 5768; (d) E.M. Glebov, A.V. Kolomeets, I.P. Pozdnyakov, V.P. Grivin, V.F. Plyusnin, N.V. Tkachenko and H. Lemmetyinen, *Russ. Chem. Bull.*, 2013, **62**, 1540; (e) I.P. Pozdnyakov, E.M. Glebov, S.G. Matveeva, V.F. Plyusnin, A.A. Melnikov and S.V. Chekalin, *Russ. Chem. Bull.*, 2015, **64**, 1784.
- 17 S.G. Matveeva, I.P. Pozdnyakov, V.P. Grivin, V.F. Plyusnin, A.S. Mereshchenko, A.A. Melnikov, S.V. Chekalin and E.M. Glebov, *J. Photochem. Photobiol. A: Chem.*, 2016, **325**, 13.
- 18 (a) A. Goursot, H. Chermette, E. Peigault, M. Chanon and W.L. Waltz, *Inorg. Chem.*, 1984, **23**, 3618; (b) A. Goursot, H. Chermette, E. Peigault, M. Chanon and W.L. Waltz, *Inorg. Chem.*, 1985, **24**, 1042; (c) A. Goursot, A.D. Kirk, W.L. Waltz, G.B. Porter and D.K. Sharma, *Inorg. Chem.*, 1987, **26**, 14; (d) A. Goursot, H. Chermette, W.L. Waltz and J. Lillie, *Inorg. Chem.*, 1989, **28**, 2241; (e) W.L. Waltz, J. Lillie, A. Goursot and H. Chermette, *Inorg. Chem.*, 1989, **28**, 2247.
- 19 L. Moggi, G. Varani, M.F. Manfrin and V. Balzani, *Inorg. Chim. Acta*, 1970, **4**, 335.
- 20 E.M. Glebov, V.F. Plyusnin, N.V. Tkachenko and H. Lemmetyinen, *Chem. Phys.*, 2000, **257**, 79.
- 21 (a) E.M. Glebov, A.V. Kolomeets, I.P. Pozdnyakov, V.F. Plyusnin, N.V. Tkachenko and H. Lemmetyinen, *Photochem. Photobiol. Sci.*, 2011, **10**, 1709; (b) E.M. Glebov, I.P. Pozdnyakov, A.A. Melnikov and S.V. Chekalin, *J. Photochem. Photobiol. A: Chem.*, 2014, **292**, 34.
- 22 C. Rensing, O.T. Ehrler, J.-P. Yang, A.-N. Unterreiner and M.M. Kappes, *J. Chem. Phys.*, 2009, **130**, 234306 (1-8).
- 23 (a) E.M. Glebov, V.P. Chernetsov, V.P. Grivin, V.F. Plyusnin and A.B. Venediktov, *Mendeleev Commun.*, 2014, **24**, 111; (b) E.M. Glebov, I.P. Pozdnyakov, V.P. Chernetsov, V.P. Grivin, A.B. Venediktov, A.A. Melnikov, S.V. Chekalin and V.F. Plyusnin, *Russ. Chem. Bull.*, 2017, **66**, 418.
- 24 E.M. Glebov, I.P. Pozdnyakov, S.G. Matveeva, A.A. Melnikov, S.V. Chekalin, M.V. Rogozina, V.V. Yudanov, V.P. Grivin and V.F. Plyusnin, *Photochem. Photobiol. Sci.*, 2017, **16**, 220.
- 25 W. Casenpusch and W. Preetz, *Z. Anorg. Allg. Chem.*, 1977, **432**, 107.
- 26 E.M. Glebov, V.F. Plyusnin, V.P. Grivin and Yu.V. Ivanov, *Russ. J. Coord. Chem.*, 1997, **23**, 580.
- 27 L.A. Pena and P.E. Hoggard, *Photochem. Photobiol.*, 2010, **86**, 467.
- 28 C.K. Jørgensen, *Mol. Phys.*, 1959, **2**, 309.
- 29 S.M. Khan, H.H. Patterson, H. Engstrom, *Mol. Phys.*, 1978, **35**, 1623.
- 30 S.V. Chekalin, *Phys. Usp.*, 2006, **49**, 634.
- 31 C.C. Lovallo and M. Klobukowski, *J. Comput. Chem.*, 2003, **24**, 1009.
- 32 C.C. Lovallo and M. Klobukowski, *J. Comput. Chem.*, 2004, **25**, 1206.
- 33 M.W. Schmidt, K.K. Baldrige, J.A. Boatz, S.T. Elbert, M.S. Gordon, J.H. Jensen, S. Koseki, N. Matsunaga, K.A. Nguyen, S.J. Su, T.L. Windus, M. Dupuis and J.A. Montgomery, *J. Comput. Chem.*, 1993, **14**, 1347.
- 34 (a) A.A. Granovsky, *J. Chem. Phys.*, 2011, **134**, 214113 (1-14); (b) FireFly Project homepage: <http://classic.chem.msu.su/gran/firefly/index.html>.
- 35 C.K. Jørgensen and W. Preetz, *Z. Naturforsch.*, 1967, **22a**, 945.
- 36 A.S. Rury and R.J. Sension, *Chem. Phys.*, 2013, **422**, 220.



Photoaquation of $\text{Os}^{\text{IV}}\text{Cl}_6^{2-}$ complex occurs via pentacoordinated $\text{Os}^{\text{IV}}\text{Cl}_5^-$ intermediate.